

# Crosstalk-aware dynamic spectrum management algorithm for green DSL systems

Chee Keong Tan<sup>1</sup> · Teong Chee Chuah<sup>1</sup> · Mohd Saiful Bahri<sup>2</sup>

Published online: 7 August 2017  
© Springer Science+Business Media, LLC 2017

**Abstract** Dynamic spectrum management (DSM) techniques mitigate crosstalk in digital subscriber line (DSL) networks by adapting the transmit spectra to the actual noise and channel conditions. Conventional DSM schemes are designed based on single-objective optimization, either belonging to the rate-adaptive or margin-adaptive category. In this paper, an efficient crosstalk-aware DSM (CA-DSM) algorithm which jointly considers both the data rate and power is proposed to search for the best rate-power tradeoff solution based on the network conditions. The crosstalk-aware power strategy prevents transmitters which contribute excessive crosstalk from being allocated high power, thereby reducing the aggregate crosstalk noise in the system. A convex cost function is used to formulate the DSM optimization problem wherein two coefficients are introduced to make the CA-DSM algorithm adaptive to different network conditions. An iterative power update strategy is proposed for the CA-DSM algorithm to minimize the cost function. Convergence properties of the CA-DSM algorithm along with existence and uniqueness of optimal power solutions are examined analytically and illustrated graphically. Simulation results show

that the proposed CA-DSM algorithm can provide a significantly better rate-power tradeoff performance compared to existing spectrum management schemes.

**Keywords** Digital subscriber line · Dynamic spectrum management · Crosstalk · Energy efficiency · Spectral efficiency

## 1 Introduction

The performance of digital subscriber line (DSL) systems is severely constrained by crosstalk due to the electromagnetic coupling among the multiple twisted pairs making up a copper cable bundle. In order to alleviate performance degradation arising from crosstalk, DSL systems adopt static spectrum management (SSM) techniques which employ identical power spectral masks for all DSL transmitters [1]. Nevertheless, conventional SSM techniques [2] are designed under the assumption of worst-case crosstalk scenarios, hence resulting in overly conservative DSL deployments [3]. A new paradigm for DSL system design is to implement dynamic spectrum management (DSM) [4] which has been envisioned as an enabling technology for crosstalk mitigation. The DSM approach overcomes the problem encountered by SSM through a mechanism of altering the spectrum of each modem to match the specific DSL network topology. These spectra are adapted according to the direct channel gains and crosstalk received by different modems.

In general, there are three levels of DSM: DSM level 1 independently performs spectrum balancing for individual line to mitigate crosstalk; DSL level 2 jointly performs spectrum balancing across multiple lines to mitigate crosstalk; and DSL level 3 performs signal-level coordination (using

✉ Chee Keong Tan  
tckeong@mmu.edu.my

Teong Chee Chuah  
tcchuah@mmu.edu.my

Mohd Saiful Bahri  
saifulbahri@tmrnd.com.my

<sup>1</sup> Faculty of Engineering, Multimedia University, Jalan Multimedia, 63100 Cyberjaya, Selangor Darul Ehsan, Malaysia

<sup>2</sup> Telekom Research & Development Malaysia Sdn Bhd, Lingkaran Teknokrat Timur, 63000 Cyberjaya, Selangor, Malaysia

vectoring schemes) to remove crosstalk. A detailed survey of DSM levels 1 and 2 is provided in [5] while survey of DSM level 3 can be found in [6]. In this work, our focus is on DSM level 2 where optimization of the transmit spectra among multiple users is performed to reduce the aggregate crosstalk noise in the DSL network. Thus far, most research efforts on DSM design have been centered around data rate maximization (i.e., rate-adaptive DSM [5]), with little emphasis on the design objective of power minimization (i.e., margin-adaptive [5]), except to fulfill the power spectral density (PSD) constraints defined by DSL standards.

One of the earliest DSM algorithms is the Iterative Water-Filling (IWF) algorithm [7], which is a distributed DSM scheme where users autonomously and selfishly maximize their own data rate. Undeniably, the IWF algorithm achieves substantial rate improvements over SSM schemes; however, in many situations, the IWF-based DSM leads to sub-optimal bit-rate performance due to poor spectral efficiency [8]. Two similar schemes which attempt to enhance the performance of IWF are Band Preference Spectrum Management (BPSM) [9] and Iterative Power Pricing (IPP) [10], both of which apply the general IWF algorithm, except that they formulate the optimization problem differently. The BPSM is designed to maximize the achievable data rate while the IPP is tasked to achieve a target rate subject to the minimal power constraints. Another algorithm known as Selective IWF (SIW) [11] addresses the performance degradation of the IWF algorithm caused by under-utilized high-frequency bands of near users in the presence of far users. Thus, the SIW algorithm selectively applies IWF to users in under-utilized frequency bands until all users have consumed their total power. Although the SIW approach outperforms the IWF, its bit-rate performance remains sub-optimal. In addition, an enhanced IWF algorithm is proposed in [12] recently to address the near-far problem in very-high-bit-rate DSL (VDSL) upstream by backing off power from subcarriers of near-end users causing the worst degradation on the bit rates of far-end users. In [13], the authors studied real-time spectrum coordination based on bi-coordinate ascent methods with provable convergence properties to improve bit-rate performance.

Recently, the DSM optimization problem has been solved using dual-decomposition based algorithms, which can achieve optimal or near-optimal performance. A centralized algorithm known as Optimal Spectrum Balancing (OSB) [14] is developed to maximize the weighted sum rate across all users. Based on dual decomposition, maximization is performed to obtain optimal power solutions for each user on every tone by exhaustive search. While the OSB scheme achieves optimal performance, it is not computationally tractable for cases with large numbers of users. To reduce its computational complexity, a similar centralized algorithm known as Grouping Spectrum Management (GSM)

[15] is introduced. This scheme partitions DSL users into different clusters based on their loop lengths and calculates a reference length for each cluster, over which the GSM applies the OSB scheme. This method is capable of tremendously reducing the complexity of the OSB at the cost of marginal performance degradation in terms of total bit rate. Besides, a low-complexity algorithm [16] based on dual-decomposition approach is developed for both linear and non-linear precoding-based DSM that maximizes the weighted sum-rate subject to the per-line total power and per-tone PSD mask constraints. Other rate-adaptive DSM schemes are discussed in [5] and the references therein.

Energy-efficient DSM is a recent prevalent topic in the DSL community, mainly motivated by the global trend to enable green communications in broadband access networks for reducing carbon footprint. To achieve this goal, international standard bodies together with researchers from industry and academia are entrusted to develop energy-efficient techniques within the scope of their activities in DSL systems while preserving the quality of DSL services. In [7], an iterative DSM algorithm is proposed to minimize the sum power for each user in a distributed manner. The DSM problem is modeled using non-cooperative game theory which leads to a near-optimal power solution known as Nash equilibrium. In [17–19], an iterative geometric programming approximation is employed to minimize the weighted aggregate transmit power (ATP) of multiuser DSL systems. Furthermore, a band-preference method is proposed in [20] to reduce power consumption and improve network stability, which influences spectrum usage through band preference factors that subtly modify the bit-loading algorithm of DSL modems. Besides, a power back-off procedure is adopted in [21] to minimize the ATP and improve the robustness of DSM against channel and noise variations. The work in [22] describes an algorithm that selects suitable upstream power back-off parameters for vectored and non-vectored lines, leading to a much lower computation requirements compared to the OSB scheme, but the achievable rates are very close to the OSB theoretical limits. Other margin-adaptive DSM schemes are presented in [5] and the references therein.

To date, most of the DSM schemes are designed based on single-objective optimization [23], which are either rate-adaptive or margin-adaptive. However, these DSM schemes may not be beneficial to DSL service providers with network objectives based on data usage or traffic trends. For example, during off-peak traffic hours, rate-adaptive DSM schemes may maximize data rate unnecessarily, leading to power wastage. On the other hand, during data-heavy hours, margin-adaptive DSM schemes may minimize power consumption excessively, resulting in increased delays and packet loss rates. Since power consumption minimization and data rate

maximization are two conflicting optimization objectives, it is essential to formulate a flexible multi-objective optimization function to control the tradeoff between these two contradictory goals [23]. In fact, both power and data rate are highly correlated with crosstalk [24], i.e., crosstalk noise increases linearly with power consumption while data rate degrades logarithmically with respect to crosstalk noise [7]. Therefore, a joint optimization of power and data rate can be performed effectively if the aggregate crosstalk noise in the DSL network is managed cautiously.

In this paper, an efficient DSM technique known as crosstalk-aware DSM (CA-DSM) algorithm is proposed to obtain the best rate-power tradeoff solution based on the downstream traffic conditions. This DSM scheme considers both power and data rate in a joint convex cost function defined with two adjustable coefficients. These coefficients play an essential role to make the CA-DSM scheme adaptive by placing different levels of emphasis on power consumption and data rate achievement. By adjusting the values of these coefficients, different network objectives (based on traffic conditions) can be achieved. Besides, the influence of crosstalk is also captured in the proposed cost function whereby DSL transmitters which contribute excessive crosstalk noise to the system will be penalized. The multi-objective optimization problem formulated is solved algebraically to obtain an optimal power updating strategy. With this strategy, the CA-DSM algorithm allocates power to every user on all the tones. Since crosstalk mitigation is embedded within this DSM scheme, a good tradeoff between energy efficiency (power consumption) and spectral efficiency (data rate achievement) can be achieved under any network conditions.

## 2 System model for DMT-based multiuser DSL networks

Consider an  $M$ -user DSL network with the customer premises equipment (CPEs) distributed at different locations from the DSL access multiplexer (DSLAM). The CPEs receive downstream data via a bundle of twisted-pair cables emanating from the DSLAM with one twisted pair connecting one of the DSLAM transmitters to one CPE. The system is assumed to adopt the frequency-division duplexing (FDD) mode where different frequency bands are used for upstream and downstream [25], thereby resulting in negligible near-end crosstalk (NEXT) [3].

DMT is employed in which the DSL spectrum is partitioned into  $N$  tones with each tone having a bandwidth of  $B_T < B_S$  while  $B_S$  is the total system bandwidth [2]. The channel gain of the twisted copper pair belonging to the  $i$ th CPE on the  $n$ th tone is denoted as  $H_i^n(f, L_i)$ , which is dependent on the loop length  $L_i$  [25]. Different CPEs experience

diverse far-end crosstalk (FEXT) effects due to different coupling loop lengths among the twisted pairs from the DSLAM transmitters. Each CPE in this system may experience FEXT from up to  $M - 1$  disturbers. The total FEXT received by each CPE depends on the individual FEXT coupling functions and transmit PSDs of the disturbers. Moreover, the  $i$ th CPE also experiences background noise on the  $n$ th tone with a PSD denoted by  $\eta_i^n$ . Compared to FEXT, the background noise is usually negligible.

In general, when  $L_i \leq L_j$ , the FEXT transfer function of the  $i$ th pair due to the  $j$ th disturber on the  $n$ th tone can be modeled as [25]

$$H_{ij}^{n,\text{FEXT}}(f, L_i) = k_{\text{XF}} \left( \frac{f}{1\text{MHz}} \right) \sqrt{\frac{L_i}{1\text{km}}} |H_i^n(f, L_i)| \quad (1)$$

where  $k_{\text{XF}}$  is a FEXT constant. On the other hand, when  $L_i > L_j$ , the FEXT transfer function of the  $i$ th pair due to the  $j$ th disturber on the  $n$ th tone is given by [25]

$$H_{ij}^{n,\text{FEXT}}(f, L_i) = k_{\text{XF}} \left( \frac{f}{1\text{MHz}} \right) \sqrt{\frac{L_j}{1\text{km}}} |H_i^n(f, L_j)| |H_i^n(f, L_i - L_j)| \quad (2)$$

The FEXT transfer functions in (1) and (2) describe the ETSI standard “1% worst case” deterministic FEXT coupling for a single disturber [26]. In essence, a deterministic FEXT model produces identical FEXT coupling for all pairs. The 1% worst case assumption is acceptable for designing the PSD masks to limit the impact of FEXT into neighboring DSL services. Nevertheless, if all the copper pairs deployed worldwide were deemed to experience the “1% worst case” FEXT coupling strength, this would negatively bias any performance gains inherent to technologies aimed at avoiding and/or mitigating FEXT dominant crosstalk. Furthermore, the actual FEXT coupling fluctuates with the frequency and changes significantly per wire-pair combination. For the purpose of fair and reliable performance evaluations, we adopt the extended ETSI stochastic FEXT model proposed in [27] which is given by

$$H_{ij}^{n,\text{ExFEXT}}(f, L_i) = |H_i^{n,\text{FEXT}}(f, L_i)| \cdot e^{j\varphi(f)} \cdot 10^{-0.05X(f)} \quad (3)$$

where  $\varphi(f)$  is a random variable modeling the channel phase dispersion which is uniformly distributed in the interval  $[0, 2\pi]$  radians. Besides,  $X(f)$  is a Gaussian random variable expressed in dB with an average  $\mu_{\text{dB}}(f)$  and a standard deviation  $\sigma_{\text{dB}}(f)$  that models the FEXT coupling channel dispersion. Apparently, the FEXT coupling effect is dependent on  $X(f)$  in which the smaller the value of  $X(f)$ , the larger is the FEXT coupling. The term  $10^{-0.05X(f)}$  can

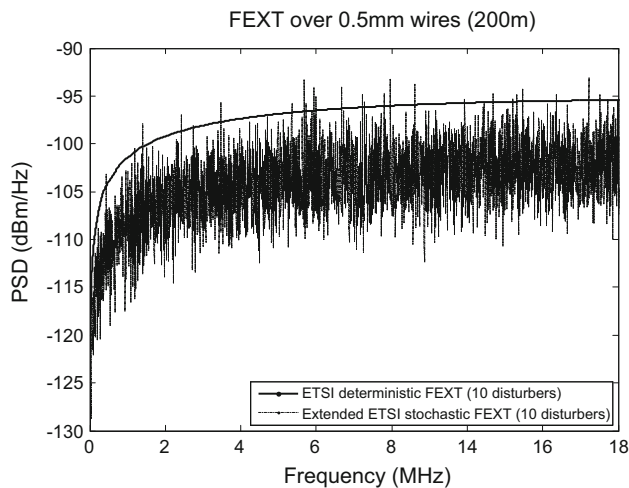


**Fig. 1** FEXT PSD simulated using the ETSI deterministic FEXT model and the extended ETSI stochastic FEXT model over a loop length of 200 m with 10 FEXT disturbers

be viewed as a modulus (magnitude) dispersion factor with respect to the standard “1% worst case” FEXT coupling, in linear scale. On the other hand,  $X(f)$  is the modulus dispersion factor with respect to the standard “1% worst case” FEXT coupling, in dB scale [25]. To utilize the extended ETSI stochastic FEXT model, it is essential to ensure that the 1% worst case value of the modulus dispersion factor is equal to “one” in the linear scale, or that the 1% worst case value of the modulus dispersion factor is equal to “zero dB”. Forcing the 1% threshold value of a Gaussian variable to 0 dB leads to the unique relationship of  $\mu_{\text{dB}} = 2.33 \times \sigma_{\text{dB}}$  [25].

A comparison of FEXT simulated using the ETSI 1% worst case deterministic FEXT model and the extended ETSI stochastic FEXT model with a dispersion of  $\sigma_{\text{dB}}(f) = 5$  dB over a 0.5 mm wire pair of length 200 m is shown in Fig. 1, where a flat transmit PSD of  $-58$  dBm/Hz is assumed to be used. If  $\sigma_{\text{dB}}(f) = 0$  dB (no dispersion), the extended ETSI stochastic FEXT model coincides with the ETSI 1% worst case deterministic FEXT model. An increasing value of  $\sigma_{\text{dB}}(f)$  reflects wider dispersion due to operating bandwidths and cable discrepancies.

Provided an adequately long cyclic prefix is used, the channel gain and noise power on each frequency tone will be flat. In this case, each tone can be modeled as an independent additive white Gaussian noise (AWGN) channel. The transmit power of the  $i$ th transmitter on the  $n$ th tone is defined as  $p_i^n$  and the signal-to-crosstalk-plus-noise ratio (SCNR) of the  $i$ th CPE on the  $n$ th tone is then given by

$$\gamma_i^n = \frac{G_{ii}^n p_i^n}{\sum_{j=1, j \neq i}^M p_j^n G_{ij}^n + \eta_i^n} \quad (4)$$

where  $G_{ii}^n = |H_i^n|^2$  and  $G_{ij}^n = |H_{ij}^{n, \text{ExFEXT}}|^2$ . The achievable bit-rate of the  $i$ th CPE on the  $n$ th frequency tone can be calculated as

$$b_i^n = \log_2 \left( 1 + \frac{G_{ii}^n p_i^n}{\Gamma \left( \sum_{j=1, j \neq i}^M p_j^n G_{ij}^n + \eta_i^n \right)} \right) \text{ bits/symbol} \quad (5)$$

where  $\Gamma$  is the overall SCNR gap from Shannon capacity for a modulation scheme at the desired error rate;  $\Gamma$  is a function of several factors, including the modulation method, allowable probability of error, channel coding gain and the desired noise margin [25]. Using (5), the achievable data rate for the  $i$ th CPE can be computed as

$$r_i = f_s \sum_{n=1}^N b_i^n \text{ bits/s} \quad (6)$$

where  $f_s$  is the DMT symbol rate. From (6), the total system data rate can be defined as

$$r_T = \sum_{i=1}^M r_i = f_s \sum_{i=1}^M \sum_{n=1}^N b_i^n \text{ bits/s} \quad (7)$$

Equation (7) is normally used as the performance metric of DSL spectral efficiency.

### 3 Crosstalk-aware dynamic spectrum management (CA-DSM) scheme

The capacity of a multipair DSL system is generally limited by FEXT. As shown in (4), one can reduce the amount of FEXT received by a CPE by lowering the transmit power of the disturbers, thereby yielding an improved SCNR and bit rate. In general, disturbers may not be willing to reduce their transmit power to avoid degrading their SCNRs [7]. Such selfish behavior generally leads to poor overall DSL system efficiency. Therefore, all DSL transceivers should compromise their individual SCNRs by jointly lowering their transmit power for an overall FEXT mitigation. Nevertheless, conventional SSM techniques adopted in current DSL networks do not possess this FEXT mitigation capability. Worse still, these SSM schemes rigidly assign power to DSL transmitters without considering their channel conditions (i.e., channel gains and FEXT coupling) on different tones, thus leading to poor energy and spectral efficiency.

To date, various DSM schemes have been proposed to overcome the limitations of SSM techniques. These DSM schemes either belong to the margin-adaptive or rate-adaptive category which emphasizes only on energy efficiency or

spectral efficiency, respectively. To the best of our knowledge, a DSM scheme which jointly considers both power and SCNR (or data rate) in the optimization objective does not exist. The current work attempts to fill this gap by devising such a DSM scheme. To achieve this goal, a cost function where both the power and SCNR can be prioritized differently to accommodate different network objectives is formulated. In view of the fact that the aggregate FEXT in the network could dramatically affect both the power consumption and SCNR achievement, an efficient CA-DSM scheme is then proposed to perform multi-objective optimization to alleviate the aggregate FEXT and to provide a good tradeoff between power and SCNR.

Since FEXT mainly arises due to excessive power usage and improper frequency planning, thus the key to improving the spectral and energy efficiency of DSL networks is to utilize network resources efficiently while minimizing FEXT. In our formulation, the influence of FEXT is captured in the cost function to prevent transmitters from introducing too much FEXT to the network by using excessive transmit power. More precisely, the FEXT-aware cost function for the  $i$ th CPE on the  $n$ th tone is formulated as

$$J_i^n = \alpha_i (\gamma_i^n - \gamma_i^{tar})^2 + \beta_i e^{\Phi_i^n (p_i^n - p_i^{tar})} p_i^n \quad (8)$$

where  $\alpha_i$  and  $\beta_i$  are adjustable non-negative coefficients. In (8),  $\gamma_i^{tar}$  and  $p_i^{tar}$  are the target SCNR and target power consumption on the  $i$ th transceiver, respectively. Besides,  $\Phi_i^n$  in (8) is a variable which is proportional to the FEXT induced by the  $i$ th transmitter to the DSL system. The term  $e^{\Phi_i^n (p_i^n - p_i^{tar})}$  is introduced as a pricing function in terms of  $\Phi_i^n$  such that transmitters which simultaneously contribute excessive FEXT and consume high power need to pay an exponential price. In this context, the price could be in the form of a fictitious credit used by the DSL service provider to govern spectrum management for the proposed CA-DSM scheme. Therefore, the main disturbing transmitters will be deterred from transmitting at high power to ensure that the aggregate FEXT in the system can be kept within an acceptable level.

Essentially, the proposed cost function should be non-negative and convex to ensure existence of a non-negative minimum solution. The second term on the right-hand side (RHS) of (8) is always positive because power consumption is always positive in any DSL application. However, the SCNR error denoted as  $(\gamma_i^n - \gamma_i^{tar})$  could be either positive or negative. To ensure positivity and convexity of the cost function, the SCNR error term on the RHS of (8) is squared in this formulation. The resulting cost function in (8) captures the tradeoff between SCNR and power consumption. The parameters  $\alpha_i$  and  $\beta_i$  allow placement of different levels of emphasis on the SCNR and power, respectively. Thus by carefully adjusting the ratio  $\alpha_i/\beta_i$  (e.g., according to the traf-

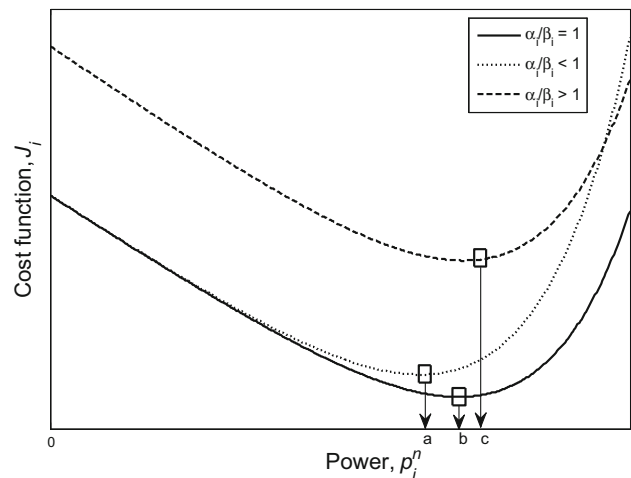


**Fig. 2** Convexity of the cost function in terms of power level to ensure a globally minimal solution for different values of  $\alpha_i/\beta_i$

fic demands), different network objectives can be achieved. For instance, if  $\alpha_i/\beta_i > 1$ , more emphasis will be placed on enhancing the SCNR while if  $\alpha_i/\beta_i < 1$ , low power usage becomes the main goal.

The objective of the current work is to propose a DSM algorithm which minimizes the cost function in (8) by adjusting the transmit power levels. To analyze the impact of  $\alpha_i/\beta_i$  on  $J_i^n$ , the relationship between the cost function and power is plotted in Fig. 2 for different values of  $\alpha_i/\beta_i$ . It is observed that for a fixed value of  $\alpha_i/\beta_i$ ,  $J_i^n$  exhibits a convex behavior and minimizing it will lead to a non-negative globally minimum power solution. In addition, it is also observed that different values of  $\alpha_i/\beta_i$  result in different power solutions. When  $\alpha_i/\beta_i = 1$ , minimizing  $J_i^n$  results in a single power solution at point ‘b’. When more emphasis is placed on SCNR, i.e.,  $\alpha_i/\beta_i > 1$ , the power solution which minimizes  $J_i^n$  is shifted to point ‘c’. Evidently, the power solution at point ‘c’ is greater than that of at point ‘b’, implying that the system is more inclined to consume more power on the  $i$ th CPE to achieve a higher SCNR. On the other hand, when  $\alpha_i/\beta_i < 1$ , implying that more emphasis is on energy efficiency, minimization of  $J_i^n$  can be achieved by a power solution at point ‘a’ which is less than those at points ‘b’ and ‘c’. Since power is the main consideration now, the SCNR might be sacrificed for a lower power consumption.

In the proposed CA-DSM scheme, the DSLAM has to allocate power efficiently to all transmitters across all tones with the objective of minimizing the aggregate cost function subject to the individual maximal power constraint. In short, the minimization problem can be expressed as

$$\min_{p_i^n} \sum_{i=1}^M \sum_{n=1}^N \left( \alpha_i (\gamma_i^n - \gamma_i^{tar})^2 + \beta_i e^{\Phi_i^n (p_i^n - p_i^{tar})} p_i^n \right) \quad (9)$$

$$\text{subject to } \sum_{n=1}^N p_i^n \leq p_i^{\max} \tag{10}$$

where  $p_i^{\max}$  is the maximum allowable transmit power for the  $i$ th transmitter. Since the cost function is convex in nature, the minimization problem in (9) can be solved algebraically to obtain a set of power solutions denoted as  $\mathbf{p}_i^* = [p_i^1, p_i^2, \dots, p_i^N]$ ,  $\forall i$ . Mathematically, the minimization problem in (9) can be solved for individual transmitters by taking the derivative of  $J_i^n$  with respect to  $p_i^n$ , i.e.,

$$\frac{\partial J_i^n}{\partial p_i^n} = 2\alpha_i (\gamma_i^n - \gamma_i^{tar}) \frac{\partial \gamma_i^n}{\partial p_i} + \beta_i e^{\Phi_i^n (p_i^n - p_i^{tar})} + \beta_i \Phi_i^n e^{\Phi_i^n (p_i^n - p_i^{tar})} p_i^n \tag{11}$$

By solving  $\partial J_i^n / \partial p_i^n = 0$  gives

$$\gamma_i^n = \gamma_i^{tar} - \frac{\beta_i e^{\Phi_i^n (p_i^n - p_i^{tar})} (1 + \Phi_i^n p_i^n)}{2\alpha_i \frac{\partial \gamma_i^n}{\partial p_i^n}} \tag{12}$$

By substituting (4) into (12) yields

$$\frac{G_{ii}^n p_i^n}{\sum_{j=1, j \neq i}^M p_j^n G_{ij}^n + \sigma_i^n} = \gamma_i^{tar} - \frac{\beta_i e^{\Phi_i^n (p_i^n - p_i^{tar})} (1 + \Phi_i^n p_i^n)}{2\alpha_i \frac{\partial \gamma_i^n}{\partial p_i^n}} \tag{13}$$

where

$$C_i(\mathbf{p}_{-i}^n) = \sum_{j=1, j \neq i}^M p_j^n G_{ij}^n + \eta_i^n \tag{14}$$

For brevity, let  $C_i(\mathbf{p}_{-i}^n)$  denote the total crosstalk-plus-noise received by the  $i$ th CPE on the  $n$ th tone, which is dependent on the power set denoted as  $\mathbf{p}_{-i}^n$ . More precisely,  $\mathbf{p}_{-i}^n$  represents the power vector containing the power of all transmitters on the  $n$ th tones except that of the  $i$ th transmitter. Substituting (14) into (13) and rearranging (13) leads to the following efficient power minimization strategy (also known as the power update method)

$$p_i^n(k+1) = \gamma_i^{tar} \left( \frac{C_i(\mathbf{p}_{-i}^n(k))}{G_{ii}^n} \right) - \frac{\beta_i \Omega(k)}{2\alpha_i} \left( \frac{C_i(\mathbf{p}_{-i}^n(k))}{G_{ii}^n} \right)^2 \tag{15}$$

where  $\Omega(k) = e^{\Phi_i^n (p_i^n(k) - p_i^{tar})} (1 + \Phi_i^n p_i^n(k))$ . Obviously, the power minimization strategy defined in (15) is an iterative power update method which requires information from the past. From (15), it is shown that the current power update strategy for the  $i$ th transmitter at the  $(k+1)$ th iteration

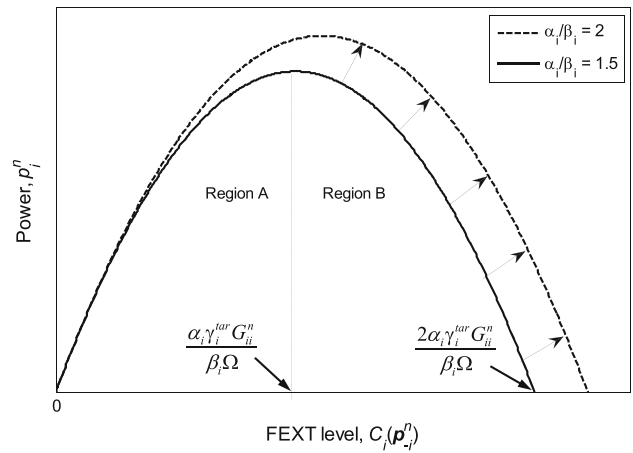


Fig. 3 Power regions for different FEXT levels and two values of  $\alpha_i/\beta_i$

depends on its power level and the FEXT induced by other disturbers at the  $k$ th iteration.

The power strategy in (15) is shown as a function of  $C_i(\mathbf{p}_{-i}^n(k))$  in Fig. 3 to illustrate its relationship with the FEXT noise, where it is noticed that the impact of the power strategy on the FEXT level can be partitioned into two regions with a boundary determined by the latter. Taking the derivative of  $p_i^n$  with respect to  $C_i$  and equate it to zero, we have

$$\frac{\partial p_i^n}{\partial C_i} = \frac{\gamma_i^{tar}}{G_{ii}^n} - \frac{\beta_i \Omega}{\alpha_i} \left( \frac{C_i(\mathbf{p}_{-i}^n)}{(G_{ii}^n)^2} \right) = 0 \tag{16}$$

Solving (16) gives the FEXT solution

$$C_i(\mathbf{p}_{-i}^n) = \frac{\alpha_i \gamma_i^{tar} G_{ii}^n}{\beta_i \Omega} \tag{17}$$

Equation (17) defines the boundary that divides the two regions shown in Fig. 3. To obtain the maximum bound for a given FEXT level, (15) is equated to zero to yield

$$\gamma_i^{tar} \left( \frac{C_i(\mathbf{p}_{-i}^n(k))}{G_{ii}^n} \right) - \frac{\beta_i \Omega(k)}{2\alpha_i} \left( \frac{C_i(\mathbf{p}_{-i}^n(k))}{G_{ii}^n} \right)^2 = 0 \tag{18}$$

Solving (18) produces the maximum bound of the FEXT as

$$C_i(\mathbf{p}_{-i}^n) = \frac{2\alpha_i \gamma_i^{tar} G_{ii}^n}{\beta_i \Omega} \tag{19}$$

The bounds defined in (17) and (19) can be used to analyze the feasibility region of the proposed power minimization strategy.

In Fig. 3, region A denotes the region for which  $0 < C_i(\mathbf{p}_{-i}^n) < \alpha_i \gamma_i^{tar} G_{ii}^n / \beta_i \Omega$ , where the FEXT level increases with respect to power. This scenario is justifiable because when a transmitter deploys more power, others will follow suit so that the SCNR would not be jeopardized,

leading to a higher aggregate FEXT level in the network. Conversely, region B denotes the region for which  $\alpha_i \gamma_i^{tar} G_{ii}^n / \beta_i \Omega < C_i (p_{-i}^n) < 2\alpha_i \gamma_i^{tar} G_{ii}^n / \beta_i \Omega$ , where the FEXT level decreases with power, signifying the infeasible region of the power minimization strategy. Therefore, region B will be ignored and it will also be proven in a latter section that the maximum allowable FEXT level received by a CPE is always less than  $\alpha_i \gamma_i^{tar} G_{ii}^n / \beta_i \Omega$ . Besides, it is also manifested in Fig. 3 that when the ratio  $\alpha_i / \beta_i$  increases from 1.5 to 2.0, region A is expanded, implying that the system can tolerate a higher FEXT level. In other words, an increase in  $\alpha_i / \beta_i$  means that the system prioritizes SCNR over power, hence the system is allowed to transmit more power to achieve the target SCNR.

#### 4 Convergence analysis of the CA-DSM algorithm

The power update method derived in (15) is an iterative strategy which is tasked to solve the minimization problem defined in (9). If the strategy in (15) is performed iteratively for all transmitters, convergence of the CA-DSM algorithm to a fixed point must always be guaranteed so that the ultimate power allocation is optimal and efficient. Furthermore, divergence of the algorithm will lead to a never-ending power update process because the results from an infeasible cost function will encourage the system to incessantly allocate impractical amount of power to the transmitters. Before studying the convergence behavior of the CA-DSM algorithm, the existence of a unique solution must first be established. In this section, the existence of a solution for the CA-DSM algebraic equation needs to be established under the same condition that guarantees the existence of solution for the power updating equation in (15). According to the Implicit Function Theorem [28], the established solution is the optimal point to which the CA-DSM algorithm tends to converge because the convergence to this optimal point minimizes the cost function in (9).

By substituting (14) into (15), the algebraic equation of the system considered is given by

$$F_i = -p_i^n + \frac{\gamma_i^{tar}}{G_{ii}^n} \left( \sum_{j=1, j \neq i}^M p_j^n G_{ij}^n + \eta_i^n \right) - \frac{\beta_i \Omega(k)}{2\alpha_i (G_{ii}^n)^2} \left( \sum_{j=1, j \neq i}^M p_j^n G_{ij}^n + \eta_i^n \right)^2 \quad (20)$$

If  $F_1, F_2, \dots, F_M$  are differential functions, a Jacobian matrix can be defined as

$$\mathcal{J}_F(p_1^n, p_2^n, \dots, p_M^n) = \begin{pmatrix} \frac{\partial F_1}{\partial p_1^n} & \frac{\partial F_1}{\partial p_2^n} & \dots & \frac{\partial F_1}{\partial p_M^n} \\ \frac{\partial F_2}{\partial p_1^n} & \frac{\partial F_2}{\partial p_2^n} & \dots & \frac{\partial F_2}{\partial p_M^n} \\ \vdots & \vdots & \ddots & \vdots \\ \frac{\partial F_M}{\partial p_1^n} & \frac{\partial F_M}{\partial p_2^n} & \dots & \frac{\partial F_M}{\partial p_M^n} \end{pmatrix} \quad (21)$$

$$= \begin{pmatrix} \nu & \frac{G_{12}^n}{G_{11}^n} (\gamma_1^{tar} - \frac{\kappa_1}{\gamma_2^n}) & \dots & \frac{G_{1M}^n}{G_{11}^n} (\gamma_1^{tar} - \frac{\kappa_1}{\gamma_M^n}) \\ \frac{G_{21}^n}{G_{22}^n} (\gamma_2^{tar} - \frac{\kappa_2}{\gamma_1^n}) & \nu & \dots & \frac{G_{2M}^n}{G_{22}^n} (\gamma_2^{tar} - \frac{\kappa_2}{\gamma_M^n}) \\ \vdots & \vdots & \ddots & \vdots \\ \frac{G_{M1}^n}{G_{MM}^n} (\gamma_M^{tar} - \frac{\kappa_M}{\gamma_1^n}) & \frac{G_{M2}^n}{G_{MM}^n} (\gamma_M^{tar} - \frac{\kappa_M}{\gamma_2^n}) & \dots & \nu \end{pmatrix} \quad (22)$$

where the main diagonal elements of the Jacobian matrix in (22) are represented by  $\nu$  which can be expressed as

$$\nu = -1 - \frac{\beta_i}{\alpha_i} \Phi_i^n e^{\Phi_i^n (p_i^n - p_i^{tar})} \left( 1 + \frac{\Phi_i^n p_i^n}{2} \right) \left( \frac{\sum_{j=1, j \neq i}^M p_j^n G_{ij}^n + \eta_i^n}{G_{ii}^n} \right)^2 \quad (23)$$

Besides,  $\kappa_i$  in (22) is given by

$$\kappa_i = \frac{\beta_i e^{\Phi_i^n (p_i^n - p_i^{tar})} (1 + \Phi_i^n p_i^n)}{\alpha_i} \quad (24)$$

According to the Implicit Function Theorem, the Jacobian matrix must be non-singular at the point of existence [28]. Apparently, it is shown in (23) that the main diagonal elements of (22) are always negative. The non-singularity of the Jacobian matrix (22) can be preserved if the off-diagonal elements of (22) are relatively small. In (22), these terms mainly depend on  $G_{ii}^n$  and  $G_{ij}^n$ . If  $G_{ij}^n$  are large enough to cause singularity in (22), the  $j$ th transmitter is turned off by deleting the  $j$ th diagonal element of the Jacobian matrix. In other words, the DSL system employing the CA-DSM algorithm punishes transmitters that induce excessive FEXT noise to the DSL network by “switching off” their transmission. Physically, these transmitters will not receive data on the affected tones to limit the aggregate FEXT to an acceptable level. This ensures that the off-diagonal terms of (22) are always small enough, and thus a unique solution for the derived algebraic equation always exists in the proposed CA-DSM algorithm.

In the above proof, it is shown that a unique solution for the proposed CA-DSM algorithm always exists. However, a power update method is required to lead the algorithm to converge to this solution. To prove that the proposed power updating method in (15) always ensures convergence of the CA-DSM algorithm, the method in [29] can be adopted. According to [29], an algorithm  $p(k+1) = f(p(k))$  always converges to a unique fixed point if the function  $f$  satisfies the following properties: (1) Positivity, i.e.,  $f(p) > 0$ ;



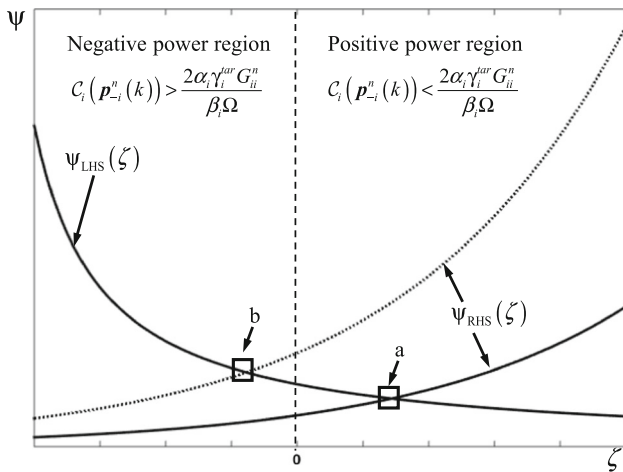


Fig. 4 Illustration of power regions under different FEXT levels

(2) Monotonicity, i.e.,  $p' > p \Rightarrow f(p') > f(p)$ ; and  
 (3) Scalability, i.e.,  $\varepsilon f(p) > f(\varepsilon p), \forall \varepsilon > 1$ . If the powers of all transmitters are updated using the power strategy derived in (15), convergence of the CA-DSM algorithm will ensure that each transmitter is allocated a fixed amount of power at the end of the updating process. Upon convergence,  $p_i^n(k) = p_i^n(k+1)$  and (15) is said to have been reduced to a transcendental equation given by

$$\frac{C_i(\mathbf{p}_{-i}^n) \gamma_i^{tar} - G_{ii}^n p_i^n}{C_i(\mathbf{p}_{-i}^n) (1 + \Phi_i^n p_i^n)} = \frac{\beta_i C_i(\mathbf{p}_{-i}^n)}{2\alpha_i G_{ii}^n} e^{\Phi_i^n (p_i^n - p_i^{tar})} \quad (25)$$

The left-hand side (LHS) of (25) can be represented as

$$\psi_{LHS}(\zeta) = \frac{C_i(\mathbf{p}_{-i}^n) \gamma_i^{tar} - G_{ii}^n \zeta}{C_i(\mathbf{p}_{-i}^n) (1 + \Phi_i^n \zeta)} \quad (26)$$

whereas the RHS of (25) can be written as

$$\psi_{RHS}(\zeta) = \frac{\beta_i C_i(\mathbf{p}_{-i}^n)}{2\alpha_i G_{ii}^n} e^{\Phi_i^n (\zeta - p_i^{tar})} \quad (27)$$

The solution to (25) is  $\zeta$  (used to represent  $p_i^n$ ) which satisfies  $\psi_{LHS}(\zeta) = \psi_{RHS}(\zeta)$ . This solution is illustrated by plotting the curves of  $\psi_{LHS}(\zeta)$  and  $\psi_{RHS}(\zeta)$  against  $\zeta$  in Fig. 4. In this figure, the intersection between  $\psi_{LHS}(\zeta)$  and  $\psi_{RHS}(\zeta)$  is at point ‘a’, which satisfies  $\psi_{LHS}(\zeta) = \psi_{RHS}(\zeta)$ . This graphical method is important for the following proof of convergence for the proposed CA-DSM algorithm.

Firstly, to ensure the positivity property of the function  $f$  given as  $f(p_i^n(k)) = p_i^n(k+1)$ , the following condition must be fulfilled.

$$p_i^n(k+1) = \gamma_i^{tar} \left( \frac{C_i(\mathbf{p}_{-i}^n(k))}{G_{ii}^n} \right) - \frac{\beta_i \Omega(k)}{2\alpha_i} \left( \frac{C_i(\mathbf{p}_{-i}^n(k))}{G_{ii}^n} \right)^2 > 0 \quad (28)$$

Rearranging (28) yields

$$C_i(\mathbf{p}_{-i}^n) < \frac{2\alpha_i \gamma_i^{tar} G_{ii}^n}{\beta_i \Omega} \quad (29)$$

Referring to Fig. 3, it is noticed that condition (29) always ensures positivity of the power strategy as denoted by regions A and B. Although region B is an infeasible region, the resulting power is still positive. If  $C_i(\mathbf{p}_{-i}^n(k))$  keeps increasing until condition (29) is violated, the power allocated to transmitters based on (15) may become negative, which is infeasible in DSL systems. This scenario is illustrated in Fig. 4 where the power is always in the positive region when condition (29) is fulfilled. Nonetheless, an increase in FEXT beyond the limit of (29) shifts up the curve of  $\psi_{RHS}(\zeta)$ , causing the solution denoted as ‘b’ to fall into the infeasible negative region. Hence, it is important to ensure a tolerable FEXT level in the system so that feasible power allocation can be performed to all transmitters.

Other than the condition stated in (29) in which the power must be non-negative, another condition is required to ensure that the power used by each transmitter is always less than  $p_i^{\max}$  as constrained by DSL standards, i.e.,

$$p_i^n(k+1) = \gamma_i^{tar} \left( \frac{C_i(\mathbf{p}_{-i}^n(k))}{G_{ii}^n} \right) - \frac{\beta_i \Omega(k)}{2\alpha_i} \left( \frac{C_i(\mathbf{p}_{-i}^n(k))}{G_{ii}^n} \right)^2 \leq p_i^{\max} \quad (30)$$

Solving the inequality in (30) yields

$$C_i(\mathbf{p}_{-i}^n(k)) \geq \frac{\alpha_i G_{ii}^n}{\beta_i \Omega} \left( \gamma_i^{tar} + \sqrt{(\gamma_i^{tar})^2 - \frac{2\beta_i \Omega p_i^{\max}}{\alpha_i}} \right) \quad (31)$$

$$C_i(\mathbf{p}_{-i}^n(k)) \leq \frac{\alpha_i G_{ii}^n}{\beta_i \Omega} \left( \gamma_i^{tar} - \sqrt{(\gamma_i^{tar})^2 - \frac{2\beta_i \Omega p_i^{\max}}{\alpha_i}} \right) \quad (32)$$

The regions defined by the boundaries in (31) and (32) are illustrated in Fig. 5, where the FEXT curve (solid line) is bounded by a power constraint between  $p_i^{\min} = 0$  and  $p_i^{\max}$ . It is observed that the FEXT conditions defined in (31) and (32) must be strictly fulfilled to lead the power strategy into feasible power regions bounded by  $0 \leq p_i^n \leq p_i^{\max}$ , as indicated by regions A and C. However, as described above, since region C exhibits a decreasing FEXT level with increasing power, it is thus an infeasible region. Hence, only region A should be considered in this context while region C is omitted. Additionally, the infeasible region B in Fig. 5 is

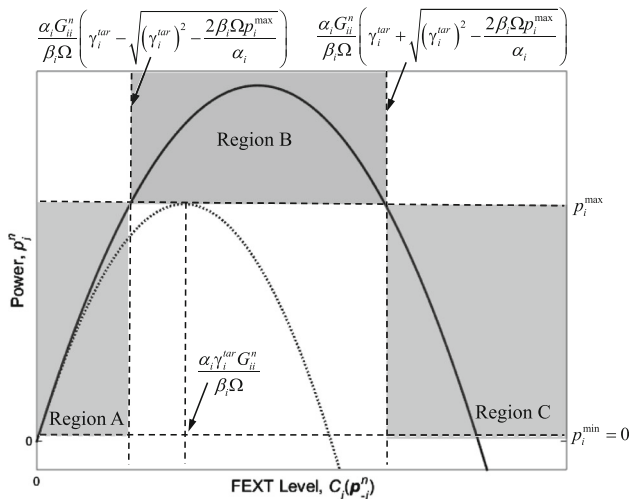


**Fig. 5** Feasible and infeasible power regions for different FEXT levels

caused by abnormal FEXT levels, thus crossing the infeasible FEXT bounds. If the FEXT level in a DSL system exceeds the infeasible bound, impractical levels of power exceeding  $p_i^{\max}$  will be allocated. Based on the illustrative example shown in Fig. 5, the infeasible region will be ignored and hence the maximum tolerable FEXT level can be simplified to condition (32) only while condition (31) can be ignored.

Moreover, it is noteworthy that the infeasible region in Fig. 5 can be minimized by reducing the ratio  $\alpha_i/\beta_i$ . The infeasible region can be eliminated entirely if

$$\sqrt{(\gamma_i^{tar})^2 - \frac{2\beta_i\Omega p_i^{\max}}{\alpha_i}} = 0 \tag{33}$$

By solving (33) results in

$$\frac{\alpha_i}{\beta_i} = \frac{2\Omega p_i^{\max}}{(\gamma_i^{tar})^2} \tag{34}$$

If condition (34) is adopted in any power updating process, the solid line in Fig. 5 will be compressed because diminishing  $\alpha_i/\beta_i$  reduces the maximum allowable transmitter power level to constrain the FEXT noise at the CPE. Therefore, as shown in Fig. 5,  $p_i^{\max}$  exactly coincides with the inflection point of the dotted line. As a result, the infeasible region is totally eliminated under this circumstance.

However, by omitting the infeasible region in the range of  $C_i(\mathbf{p}_{-i}^n) > \alpha_i\gamma_i^{tar}G_{ii}^n/\beta_i\Omega$ , the condition defined in (29) will no longer be strict enough and needs to be revised. Referring to Figs. 3 and 5, a stricter condition for the FEXT level is given by

$$C_i(\mathbf{p}_{-i}^n) < \frac{\alpha_i\gamma_i^{tar}G_{ii}^n}{\beta_i\Omega} \tag{35}$$

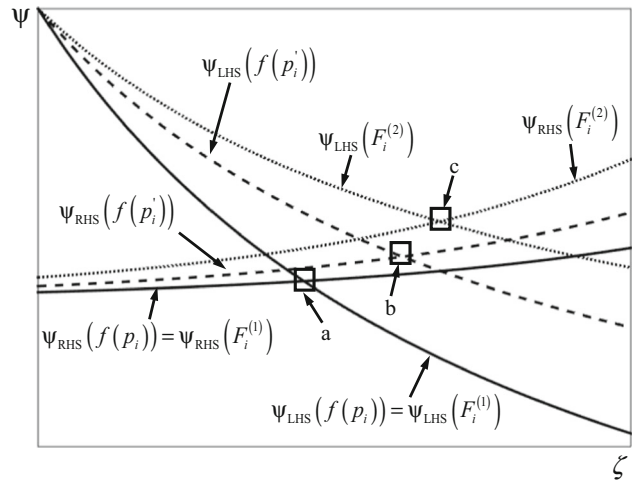


**Fig. 6** Illustration of power solutions to prove the monotonicity and scalability properties of the proposed power updating function

Any FEXT level violating the condition defined in (35) will lead to an impractical power solution and a FEXT mitigation strategy is required, which will be discussed later.

After showing the positivity property of the proposed updating function and the conditions to ensure feasible power bounds, a proof for the monotonicity property of the updating function in the CA-DSM algorithm will be provided next. Replacing  $p_i^n$  in (25) with  $f(p_i^n)$  yields

$$\frac{C_i(\mathbf{p}_{-i}^n)\gamma_i^{tar} - G_{ii}^n f(p_i^n)}{C_i(\mathbf{p}_{-i}^n)(1 + \Phi_i^n f(p_i^n))} = \frac{\beta_i C_i(\mathbf{p}_{-i}^n)}{2\alpha_i G_{ii}^n} e^{\Phi_i^n (f(p_i^n) - p_i^{tar})} \tag{36}$$

The value  $f(p_i^n)$  which satisfies (36) can be found from Fig. 6, i.e., the intersection of  $\psi_{LHS}(f(p_i^n))$  and  $\psi_{RHS}(f(p_i^n))$  at point ‘a’ is a valid solution for (36). In fact, an increase from  $p_i^n$  to  $(p_i^n)'$  results in the following scenario

$$(p_i^n)' > p_i^n \Rightarrow (\mathbf{p}_{-i}^n)' > \mathbf{p}_{-i}^n \Rightarrow C_i((\mathbf{p}_{-i}^n)') > C_i(\mathbf{p}_{-i}^n) \tag{37}$$

Note that  $0 < C_i(\mathbf{p}_{-i}^n) < 1$ , an increase from  $p_i^n$  to  $(p_i^n)' > p_i^n$  shifts up both the curves  $\psi_{LHS}(f((p_i^n)'))$  and  $\psi_{RHS}(f((p_i^n)'))$  with respect to  $\psi_{LHS}(f(p_i^n))$  and  $\psi_{RHS}(f(p_i^n))$ , respectively (cf. Fig. 6). Thus,  $f((p_i^n)')$  which satisfies  $\psi_{LHS}(f((p_i^n)')) = \psi_{RHS}(f((p_i^n)'))$  is the intersection point ‘b’. Obviously, it is shown in Fig. 6 that point ‘b’ is located at the RHS of point ‘a’, indicating that  $f((p_i^n)') > f(p_i^n)$ . Using this illustrative proof, the mono-

tonicity property of the power updating function has been verified given that  $(p_i^n)' > p_i^n \Rightarrow f((p_i^n)') > f(p_i^n)$ .

With the aid of Fig. 6, the scalability property of the updating function, i.e.,  $\varepsilon f(p) > f(\varepsilon p), \forall \varepsilon > 1$ , can be proven by first showing the following inequalities

$$\sum_{j=1, j \neq i}^M \varepsilon p_j^n G_{ij}^n + \varepsilon \sigma_i^n > \sum_{j=1, j \neq i}^M p_j^n G_{ij}^n + \sigma_i^n, \quad \forall \varepsilon > 1$$

$$\varepsilon C_i(p_{-i}^n) > C_i(\varepsilon p_{-i}^n), \quad \forall \varepsilon > 1$$
(38)

Substituting  $f(\varepsilon p_i^n)$  into (25) produces

$$\frac{C_i(\varepsilon p_{-i}^n) \gamma_i^{tar} - G_{ii}^n F_i^{(1)}}{C_i(\varepsilon p_{-i}^n) (1 + \Phi_i^n F_i^{(1)})} = \frac{\beta_i C_i(\varepsilon p_{-i}^n)}{2\alpha_i G_{ii}^n} e^{\Phi_i^n (F_i^{(1)} - p_i^{tar})}$$
(39)

where  $F_i^{(1)} = f(\varepsilon p_i^n)$ . Similarly, substituting  $\varepsilon f(p_i^n)$  into (25) yields

$$\frac{\varepsilon C_i(p_{-i}^n) \gamma_i^{tar} - G_{ii}^n F_i^{(2)}}{\varepsilon C_i(p_{-i}^n) (1 + \Phi_i^n F_i^{(2)})} = \frac{\beta_i \varepsilon C_i(p_{-i}^n)}{2\alpha_i G_{ii}^n} e^{\Phi_i^n (F_i^{(2)} - p_i^{tar})}$$
(40)

where  $F_i^{(2)} = \varepsilon f(p_i)$ . Assuming that  $\psi_{LHS}(f(p_i^n))$  and  $\psi_{RHS}(f(p_i^n))$  share the same curves with  $\psi_{LHS}(F_i^{(1)})$  and  $\psi_{RHS}(F_i^{(1)})$ , respectively as shown in Fig. 6, the solution  $F_i^{(1)}$  which satisfies  $\psi_{LHS}(F_i^{(1)}) = \psi_{RHS}(F_i^{(1)})$  is at the intersection point 'a'. Comparing (39) and (40), the curves of  $\psi_{LHS}(F_i^{(2)})$  and  $\psi_{RHS}(F_i^{(2)})$  are shifted up because  $\varepsilon C_i(p_{-i}^n) > C_i(\varepsilon p_{-i}^n)$ . Hence, the solution that satisfies  $\psi_{LHS}(F_i^{(2)}) = \psi_{RHS}(F_i^{(2)})$  is at the intersection point 'c' which is located at the RHS of point 'a', indicating  $F_i^{(2)} > F_i^{(1)} \Rightarrow \varepsilon f(p_i) > f(\varepsilon p_i)$ . This proves that the scalability property of the power updating function is always guaranteed in this algorithm.

As demonstrated above, the proposed power updating strategy always leads the CA-DSM algorithm to a set of unique power solutions for all transmitters provided the conditions defined above are strictly adhered to. For instance, if the FEXT level increases such that the condition specified in (35) is violated, the CA-DSM algorithm may not converge, resulting in impractical power allocation. As a result, the ratio  $\alpha_i/\beta_i$  needs to be adjusted so that a lower target SCNR can be achieved with less transmission power to bring down the aggregate FEXT to an acceptable level. Besides, if the SCNR is given the highest priority and cannot be compromised,

transmitters that introduce excessive FEXT to the system on the affected tones can be turned off.

### 5 The proposed CA-DSM algorithm

Figure 7 shows the proposed CA-DSM algorithm, which can lead to a set of optimal power solutions for all DSL transmitters. Since it is preferable to allocate powers to the low-frequency bands due to higher channel gains, the CA-DSM algorithm can be executed sequentially on each tone starting from low- to high-frequency bands for all transmitters to shorten convergence time. It is observed in Fig. 7 that the proposed CA-DSM algorithm is tasked to (1) acquire the channel state information (CSI); (2) estimate the aggregate FEXT in the system, and (3) iteratively update the power of all transmitters. For example, the standard-compliant DSL channel estimator described in [30] can be used to obtain

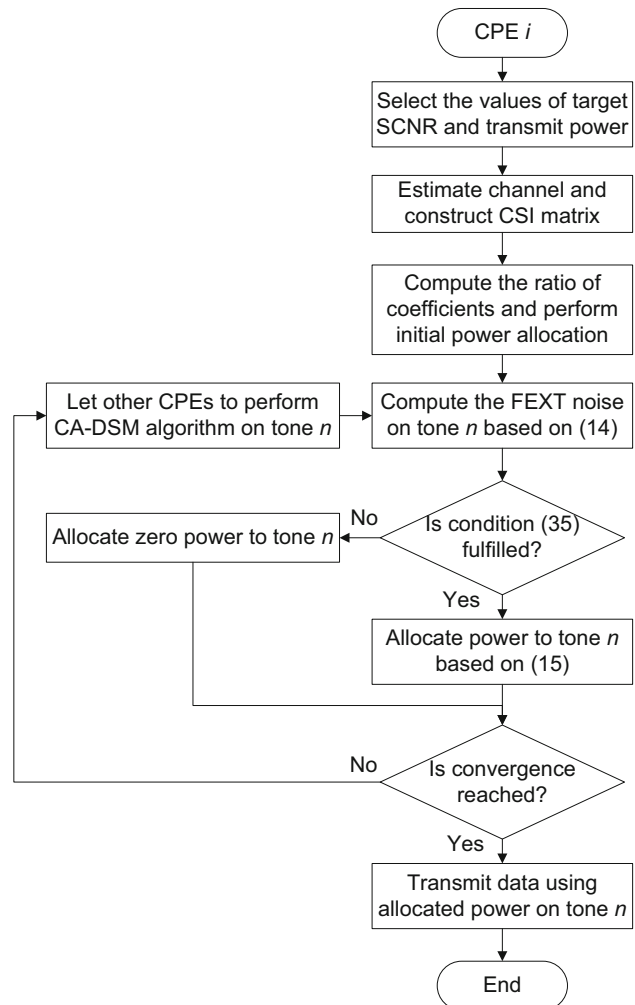


Fig. 7 Flowchart of the CA-DSM algorithm for the  $n$ th tone of an  $M$ -user DSL system

the square-magnitude of the FEXT channels, thus forming the diagonal elements  $[\mathbf{G}]_{ij} = G_{ij}^n$ . The channel estimator requires no modifications on the existing CPEs and only uses the measurement data acquired via existing DSL protocols. Using the estimated CSI matrix  $\mathbf{G}$ , the FEXT generated and received by each CPE can be estimated accordingly. If the estimated FEXT received by the  $i$ th CPE on the  $n$ th tone violates the condition given in (35), transmission to the  $i$ th CPE on the  $n$ th tone will be temporarily turned off by setting  $p_i^n = 0$ ; this reduces the aggregate FEXT in the system.

After reducing FEXT via transmitter turn offs, some transmitters may have the opportunity to regain power because less FEXT is received. If the FEXT levels are within the acceptable range, the power of all the transmitters will be updated using (15). After the power update is done, FEXT estimation is performed again to assess the FEXT level before further power updates. This process will be iteratively executed until convergence is achieved. Hence, a convergence test will be performed after every iteration by computing  $\vartheta_i^n = p_i^n(k+1) - p_i^n(k)$  until  $\vartheta_i^n < \vartheta$ , a condition in which convergence is deemed to have been achieved. As proven above, the power updating equation is convergent and therefore it is observed that  $\vartheta_i^n$  is a decreasing function of iteration. In this work,  $\vartheta$  is defined as 0.5% of the steady-state values of all transmitters' power solutions. In other words, when the power levels of all the transmitters in the DSL system fluctuate within 0.5% of their steady-state values, the algorithm is deemed to have achieved convergence. In this simulation, the selection of 0.5% is to ensure that the CA-DSM algorithm can reach its near-optimal state. If  $\vartheta$  is set larger than 0.5%, the performance of the algorithm will also be compromised though the convergence time will be shortened. Once convergence is attained, the DSLAM obtains an optimal power solution set denoted as  $p_i^*$  which is then used to transmit data to the  $i$ th CPE on all tones.

Figure 7 shows that every iteration of the CA-DSM algorithm requires  $K$  evaluations of functions (14) and (15) for FEXT and power computation on the  $n$ th tone, respectively. Therefore, the computational complexity of the CA-DSM algorithm for one iteration is  $\mathcal{O}(KN)$  where  $\mathcal{O}$  is the Bachmann–Landau big  $\mathcal{O}$  notation. Since the complexity scales linearly with the number of CPEs and tones, the CA-DSM algorithm is a low-complexity DSM scheme, which facilitates practical implementation even in DSL systems with large number of CPEs and tones.

## 6 Simulation Results

Without loss of generality, we assess the performance of the proposed CA-DSM algorithm in a VDSL2 network based on profile 17a [31] with loop lengths up to 1 km; other relevant parameters are summarized in Table 1 [32]. The initial power

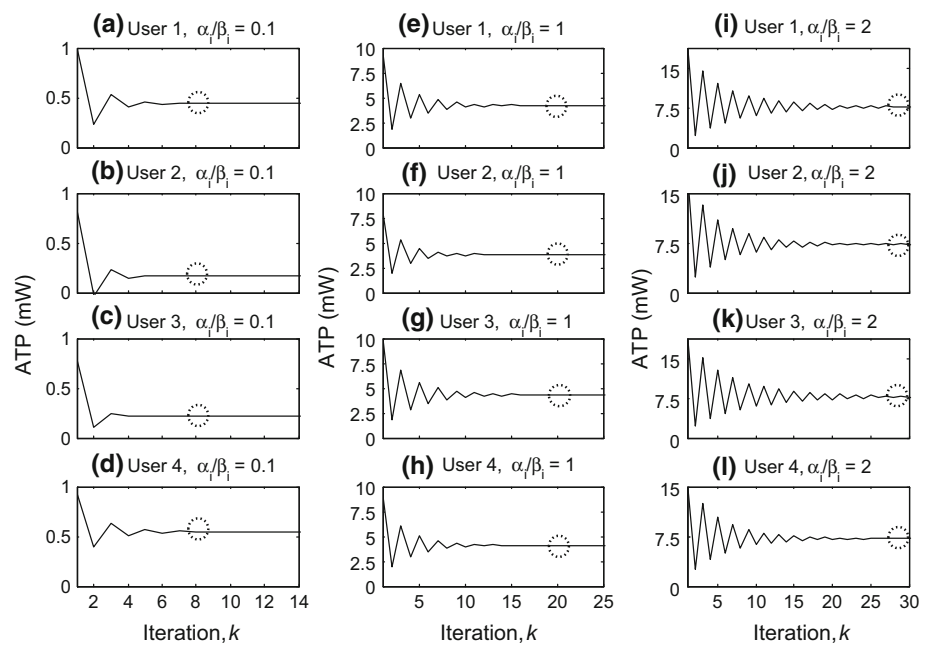
**Table 1** Simulation parameters of VDSL2 (17a)

Parameter	VDSL2 (17a)
Standard	ITU-T G.993.2 profile 17a
Bandwidth	17.664 MHz
Line coding	DMT
Number of tones	4096
Tone spacing	4.3125 kHz
Number of bits/sub-carrier	Min = 0, max = 15
Symbol rate	4000 symbols/s
Noise margin	6 dB
Coding gain	3 dB
Shannon gap	9.75 dB
Overall SCNR gap $\Gamma$	$9.75 + 6 - 3 = 12.75$ dB
Symbol error probability	$< 10^{-7}$
FEXT model	Extended ETSI stochastic model
PSD Level of background noise	-140 dBm/Hz
Wire diameter	0.5 mm

level of every transmitter is selected randomly within the power condition denoted in (10). The target SCNR and target power are set at  $\gamma_i^{tar} = 18$  dB (to ensure good signal with no sync problem) and  $p_i^{tar} = -5$  dBm (to ensure low power consumption) for all  $i$ , respectively. Besides,  $\Phi_i^n$  is adjusted linearly with respect to the FEXT level induced by the  $i$ th transmitter on the  $n$ th tone.

First, the CA-DSM algorithm is simulated in a 4-user VDSL2 network. The ATP convergence curves of the four transmitters are illustrated in Fig. 8 for different values of  $\alpha_i/\beta_i$ . In Fig. 8a–d where  $\alpha_i/\beta_i = 0.1$  is adopted, it is observed that all the ATP levels fluctuate within the threshold  $\vartheta$  and the CA-DSM algorithm converges to a set of optimal power solutions at the 8th iteration. Noticeably, the ATP levels of the four transmitters are considerably low and are  $< 0.6$  mW, implying that the pre-determined ratio of  $\alpha_i/\beta_i = 0.1$  attempts to minimize power consumption by reducing the gap between the target power and the actual power usage. Moreover, Fig. 8e–h show the results for  $\alpha_i/\beta_i = 1$ , where the CA-DSM algorithm converges slower at the 18th iteration. In this scenario, the ratio  $\alpha_i/\beta_i = 1$  enforces the DSL system to achieve certain degree of  $\gamma_i^{tar}$  while ensuring acceptable power usage. As a result, higher initial powers are allocated to all transmitters, leading to larger fluctuations which require a longer settling time. Furthermore, the converged ATP solutions are shown to be higher (at slightly  $< 5$  mW) compared to those of with  $\alpha_i/\beta_i = 0.1$ , as for now, both energy efficiency and bandwidth efficiency are equally important. When  $\alpha_i/\beta_i$  is further increased to 2 to put more emphasis on bandwidth efficiency, it is observed in Fig. 8i–l that all transmitters are allocated high ATP (of approximately 7.5 mW) after convergence of the CA-DSM algorithm. This

**Fig. 8** ATP convergence curves of 4 transmitters in a DSL system with different values of  $\alpha_i/\beta_i$



is to ensure that the target SCNR is always achieved regardless of the energy efficiency.

Next, the impact of channel conditions (i.e., channel gains and FEXT level) on the CA-DSM scheme is investigated in Fig. 9 for different values of  $\alpha_i/\beta_i$ . In the simulation, a 2-user DSL system is considered, where the loop length of transmitter 1 is fixed at 100 m whereas the loop length of transmitter 2 is varied from 500 to 900 m. The loop length variations explicitly change the channel conditions of transmitter 2 and the resulting impacts on the CA-DSM scheme are observed. In Fig. 9a–c, the use of  $\alpha_i/\beta_i = 0.1$  in the CA-DSM algorithm restricts the power consumption of transmitter 2 and this phenomenon can be observed where plenty of tones are being “switched off” (allocated zero power). When the loop length of transmitter 2 is fixed at 500 m, we notice that its power allocation is merely concentrated on tones at the high-frequency band. In this scenario, transmitter 1 which dominates tones in the low- and medium-frequency bands generates strong FEXT to CPE 2. As a result, the CA-DSM scheme enables efficient power allocation to mitigate FEXT by turning off tones that hardly improve CPE 2’s data rate.

While the loop length of transmitter 2 gradually increases, it is interesting to observe that the power allocation has shifted from the high-frequency band to the medium- and parts of low-frequency bands. Evidently, the loop length increase aggravates the channel conditions of transmitter 2 and the low value of  $\alpha_i/\beta_i$  prevents transmitter 2 from increasing power in the high-frequency band. One way to maintain CPE 2’s data rate is to shift transmitter 2’s power to the tones with better channel conditions, which are normally located in the low- and medium-frequency bands. When  $\alpha_i/\beta_i$  is increased, it is observed in Fig. 9d–i that more tones

are “activated” because the system is allowed to utilize more power, thus some tones with fair channel conditions are also allocated some power to improve the data rate of CPE 2. Besides, it is illustrated again in Fig. 9d–i that loop length can affect power allocation over different tones in different frequency bands.

Figure 10 highlights the importance of appropriate selection of  $\alpha_i/\beta_i$  on energy efficiency and spectral efficiency for different network sizes. Apparently, a decreasing value of  $\alpha_i/\beta_i$  drives the DSL system towards achieving higher energy efficiency. Therefore, it is observed in Fig. 10a that the total ATP (summation of all transmitters’ ATP) of the DSL system rises sharply with the ratio  $\alpha_i/\beta_i$ . Furthermore, the total downstream data rate also records a growing trend with the ratio  $\alpha_i/\beta_i$ , as illustrated in Fig. 10b. This phenomenon has been previously explained where a higher value of  $\alpha_i/\beta_i$  leads to higher data rate achievement albeit with more power consumption. Besides, it is also noticed in Fig. 10 that a higher ATP is required for each user in a larger network in order to achieve similar per-user data rates compared to a smaller network because more power is needed to mitigate the stronger FEXT encountered in larger networks. From Fig. 10, it can be concluded that an appropriate choice of  $\alpha_i/\beta_i$  can result in good tradeoffs between data rate achievement and power consumption for different network sizes.

In Fig. 11, the tradeoff between the average ATP and average SCNR for 10 users is investigated under different FEXT levels. The severity of FEXT in the system is controlled by randomly simulating the loop lengths of the 10 twisted pairs up to  $L_{\max}$ . In the simulation, the smaller the value of  $L_{\max}$ , the stronger is the FEXT received by the system. When  $L_{\max} = 1000$  m, the FEXT level is relatively low and

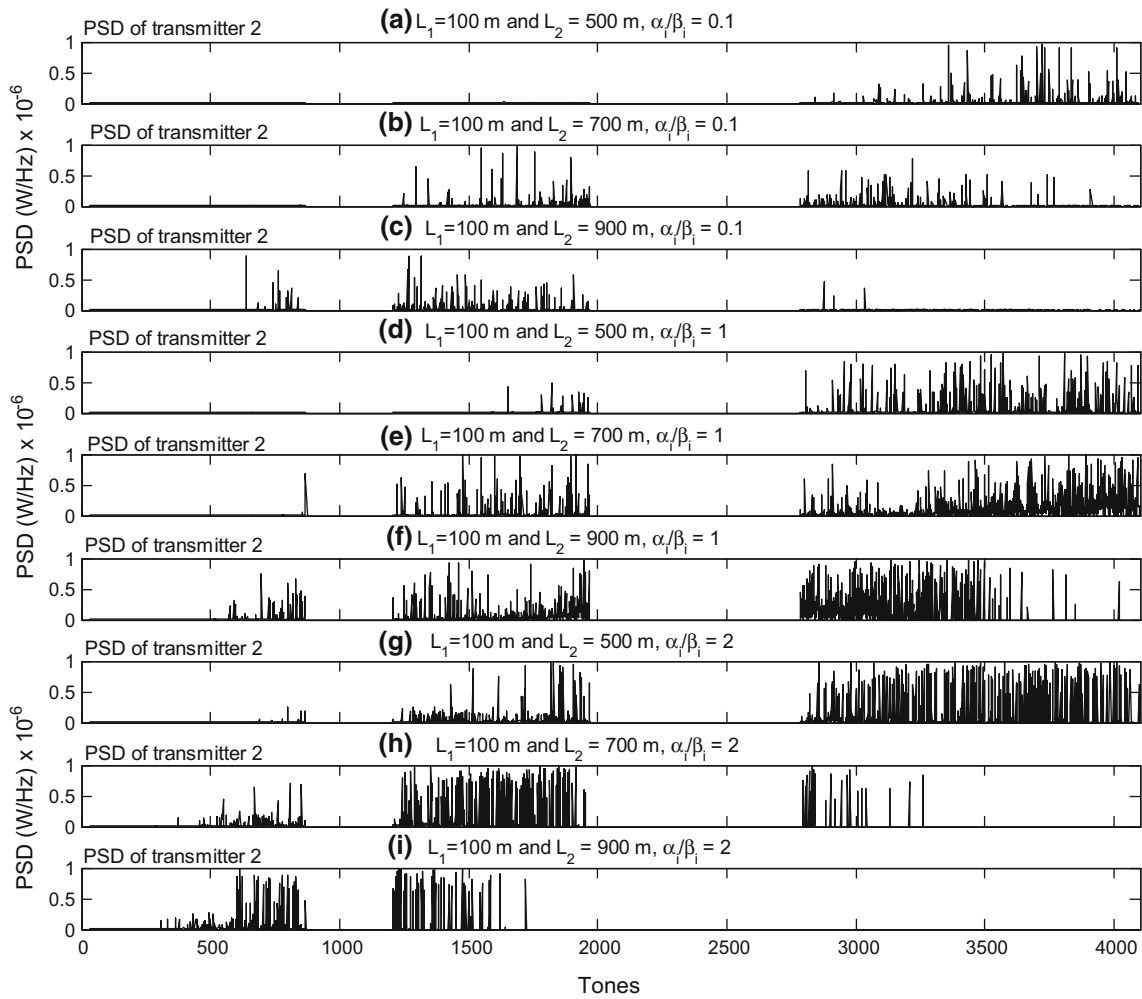


Fig. 9 Impact of channel conditions on the power allocation for transmitter 2 in a 2-user DSL network with different values of  $\alpha_i / \beta_i$

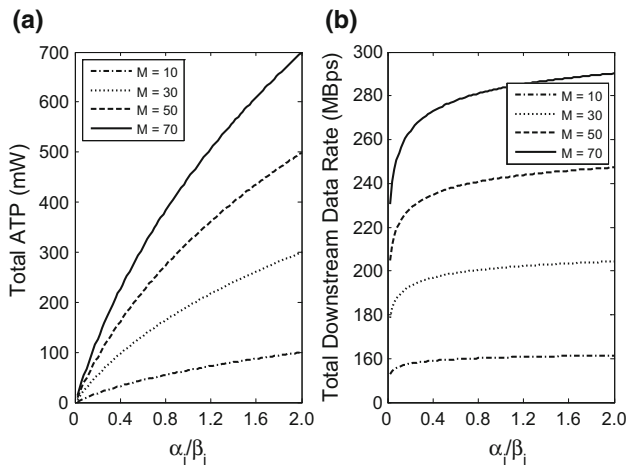


Fig. 10 Impact of  $\alpha_i / \beta_i$  on a total ATP (summation of all users' ATP); and b total downstream data rate of a DSL network with different number of users  $M$

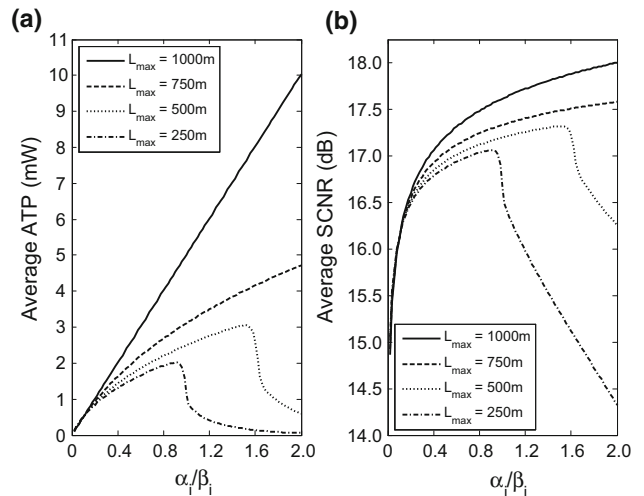
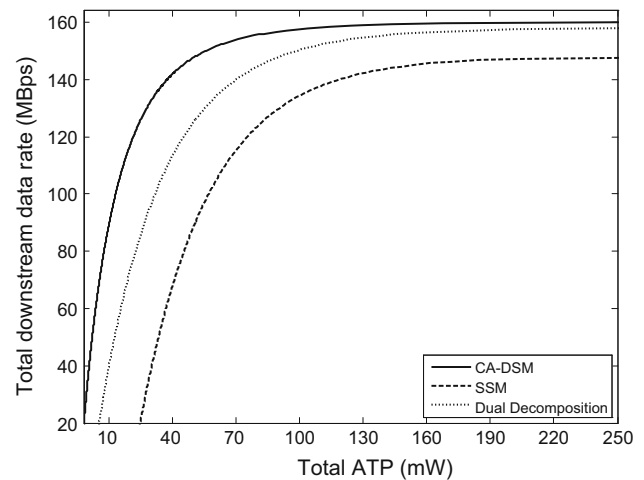


Fig. 11 Tradeoff between power reduction and SCNR degradation in a 10-user DSL network for different FEXT levels

all transceivers jointly achieve  $\gamma_i^{tar} = 18$  dB with each consuming an ATP of 10 mW as shown in Fig. 11. It is noticed that the DSL system can achieve significant power savings at a slightly degraded SCNR. For instance, a selection of  $\alpha_i/\beta_i = 1$  can reduce the average ATP by 50% at the cost of only 2.8% drop in the average SCNR. Furthermore, if the CPEs can accept a much lower average SCNR, more significant power savings can be made. By having  $\alpha_i/\beta_i = 0.2$ , the average SCNR achieved is merely 11% below  $\gamma_i^{tar}$  but an 88% power consumption reduction is recorded.

When  $L_{max} = 750$  m, jointly achieving  $\gamma_i^{tar} = 18$  dB is no longer feasible for the 10-user system due to the higher FEXT level. Consequently, only an SCNR of 17.5 dB with lower power consumption is attained. If the FEXT level is further elevated, the ATP and SCNR curves will exhibit a sudden drop for  $L_{max} = 250$  and  $L_{max} = 500$  m, as depicted in Fig. 11. The occurrence of this anomaly is due to the unsustainability of the DSL system. In other words, the 10 transceivers can no longer jointly achieve  $\gamma_i^{tar} = 18$  dB even if the system operates at maximum power. As a result, many tones have to be switched off, yielding an abrupt drop in power and SCNR. Under this circumstance, increasing the value of  $\alpha_i/\beta_i$  does not lead to SCNR enhancement, but instead may result in further SCNR degradation due to higher ATP and hence more dominant FEXT, thus depriving the system from using more tones for transmission. It is worth-mentioning that the same observation is also made in larger networks serving more users except that the ATP and SCNR curves decay sharply at lower values of  $\alpha_i/\beta_i$ . This is because the DSL system becomes increasingly unsustainable in larger networks due to higher levels of FEXT, hence the users in these networks can only achieve a lower target SCNR.

Lastly, the CA-DSM, SSM and dual-decomposition schemes are simulated and compared in terms of rate-power tradeoff in the 10-user DSL system. In Fig. 12, the total downstream system data rate versus the total ATP is demonstrated. It is noticed in Fig. 12 that the CA-DSM scheme achieves the best rate-power tradeoff among the three schemes. For a target total downstream data rate of 100 Mbps, the DSL system using the CA-DSM scheme only consumes a total ATP of 10 mW, unlike the systems adopting the SSM and dual decomposition schemes which require 55 and 25 mW, respectively. In addition, the CA-DSM scheme can achieve the best total data rate of 160 Mbps with a total ATP consumption of 130 mW whereas the dual decomposition technique consumes 160 mW to achieve the best data rate of 155 Mbps, while the SSM scheme requires 200 mW to attain a lower best data rate of 148 Mbps. Conclusively, the CA-DSM scheme outperforms the SSM and dual decomposition techniques in terms of energy and spectral efficiency, particularly in a FEXT-limited DSL environment.



**Fig. 12** Comparison of rate-power tradeoff among three schemes: CA-DSM, SSM and DSM based on dual decomposition

## 7 Conclusion

Existing DSM techniques belonging either to the rate-adaptive or margin-adaptive category may not be beneficial in DSL systems with highly varying traffic. Therefore, the DSM technique should be formulated as a multi-objective optimization to achieve optimal rate-power tradeoff. In the current work, based on a convex cost function, the adaptive CA-DSM algorithm is proposed to jointly optimize power and data rate. The optimization problem formulated is solved using an efficient power updating strategy which can lead the CA-DSM algorithm to an optimal and unique power solution. Besides, the conditions to ensure convergence of the CA-DSM algorithm have been established with the importance of the ratio  $\alpha_i/\beta_i$  highlighted. It is shown via simulation that the proposed CA-DSM algorithm is convergent if the FEXT level received is below a predefined threshold. If the ratio  $\alpha_i/\beta_i$  is chosen appropriately based on traffic demands, a remarkable improvement in power-rate tradeoff can be obtained. In addition, the CA-DSM algorithm is capable of significantly reducing power consumption at the expense of a slight degradation in data rate. In this work, we have studied the CA-DSM algorithm for non-vectorized DSL systems, but its performance in vectorized DSL is not investigated. The development of joint level 2 and 3 DSM by extending the CA-DSM algorithm for jointly obtaining the optimal precoding matrix and transmit powers for downstream transmission would be a very interesting problem for future research.

**Acknowledgements** This work was funded by Telekom Malaysia Berhad under the research grant TMRND/M/RFQ-02/2015.

## References

1. Witold, A. K., & Thomas, D. B. (2007). Performance evaluation study of signal design and equalization options for high-bit-rate digital subscriber line transceivers. *International Journal Communications Systems*, 5(1), 15–28.
2. Lee, J., Chung, S. T., & Cioffi, J. M. (2006). Optimal discrete bit-loading for DMT-based DSL systems with equal-length loops. *IEEE Transaction on Communications*, 54(10), 1760–1764.
3. ANSI Standard T1.417-2001 (2001). Spectrum management for loop transmission systems.
4. Starr, T., Sorbara, M., Cioffi, J. M., & Silverman, P. J. (2003). *DSL Advances*. New Jersey: Prentice-Hall.
5. Huberman, S., Leung, C., & Le-Ngoc, T. (2010). Dynamic spectrum management (DSM) algorithms for multi-user xDSL. *IEEE Communications Surveys & Tutorials*, 14(1), 109–130.
6. Leung, C., Huberman, S., Khuong, H., & Tho, L. (2013). Vectored DSL: potential, implementation issues and challenges. *IEEE Communications Surveys & Tutorials*, 15(4), 1907–1923.
7. Yu, W., Ginis, G., & Cioffi, J. M. (2002). Distributed multiuser power control for digital subscriber lines. *IEEE Journal on Selected Areas in Communications*, 20(5), 1105–1115.
8. Liu, Y., & Su, Z. (2007). Distributed dynamic spectrum management for digital subscriber lines. *IEICE Transactions on Communications*, E90B(3), 491–498.
9. Lee, W., Kim, Y., Brady, M. H., & Cioffi, J. M. (2006). Band-preference dynamic spectrum management in a DSL environment. In *IEEE global telecommunication conference (GLOBECOM 2006)* (pp. 1–5).
10. Noam, Y., & Leshem, A. (2009). Iterative power pricing for distributed spectrum coordination in DSL. *IEEE Transaction on Communications*, 57(4), 948–953.
11. Xu, Y., Panigrahi, S., & Le-Ngoc, T. (2007). Selective iterative water-filling for digital subscriber lines (DSL). *EURASIP Journal on Applied Signal Processing*, 2007, 1–11.
12. Sharma, S., & Sahu, P. (2016). A dynamic spectrum management algorithm in VDSL systems. *Turkish Journal of Electrical Engineering & Computer Sciences*, 2016(24), 3483–3491.
13. Verdyck, J., Blondia, C., & Moonen, M. (2016). Derivative based real-time spectrum coordination for DSL. In *European signal processing conference (EUSIPCO 2016)* (pp. 305–309).
14. Cendrillon, R., Yu, W., Moonen, M., Verlinden, J., & Bostoen, T. (2006). Optimal multiuser spectrum management for digital subscriber lines. *IEEE Transaction on Communications*, 54(5), 922–933.
15. Wei, S., Youming, L., & Miaoliang, Y. (2009). Low-complexity grouping spectrum management in multi-user DSL networks. In *IEEE international conference on communications and mobile computing (CMC 2009)* (pp. 381–385).
16. Lanneer, W., Tsiafalakis, P., Maes, J., & Moonen, M. (2017). Linear and nonlinear precoding based dynamic spectrum management for downstream vectored G.fast transmission. *IEEE Transaction on Communications*, 65(3), 1247–1259.
17. Wolkerstorfer, M., Statovci, D., & Nordström, T. (2008). Dynamic spectrum management for energy-efficient transmission in DSL. In *11th IEEE international conference on communication system* (pp. 1015–1020).
18. Nordström, T., Wolkerstorfer, M., & Statovci, D. (2009). Energy efficient power back-off management for VDSL2 transmission. In *European signal processing conference (EUSIPCO 2009)* (pp. 2097–2101).
19. Monteiro, M., Lindqvist, N., & Klautau, A. (2009). Spectrum balancing algorithms for power minimization in DSL networks. In *IEEE international conference on communications (ICC 2009)* (pp. 1–5).
20. Guenach, M., Nuzman, C., Maes, J., & Peeters, M. (2009). On power optimization in DSL systems. In *IEEE international conference on communications (ICC 2009)* (pp. 1–5).
21. Cioffi, J. M., Jagannathan, S., Lee, W., Zou, H., Chowdhery, A., Rhee, W., Ginis, G., & Silverman, P. (2008). Greener copper with dynamic spectrum management. In *IEEE global telecommunication conference (GLOBECOM 2008)* (pp. 1–5).
22. Chen, M., Ginis, G., & Mohseni, M. (2014). Dynamic upstream power back-off for mixtures of vectored and non-vectored VDSL. In *IEEE international conference on acoustics, speech and signal processing (ICASSP 2014)* (pp. 1–5).
23. Hoang, T. (1998). *Convex analysis and global optimization*. Norwell: Kluwer Academic Publishers.
24. Cendrillon, R., Huang, J. W., Chiang, M., & Moonen, M. (2007). Autonomous spectrum balancing for digital subscriber lines. *IEEE Transactions on Signal Processing*, 55(8), 4241–4257.
25. Golden, P., Dedieu, H., & Jacobsen, K. S. (2006). *Fundamentals of DSL technology*. Boca Raton: Auerbach.
26. ETSI TR 101 830-2. (2008). Transmission and multiplexing (TM); access networks; spectral management on metallic access networks; Part 2: Technical methods for performance evaluations.
27. Sorbara, M., Duvaut, P., Shmulyian, F., Singh, S., & Mahadevan, A. (2007). Construction of a DSL-MIMO channel model for evaluation of FEXT cancellation systems in VDSL2. In *IEEE Sarnoff symposium* (pp. 1–6).
28. Ortega, J. M., & Rheinboldt, W. C. (1970). *Iterative solution of nonlinear equations in several variables*. New York: Academic Press.
29. Yates, R. D. (1995). A framework for uplink power control in cellular radio systems. *IEEE Journal on Selected Areas in Communications*, 13(7), 1341–1347.
30. Lafata, P., & Jareš, P. (2008). Increasing the transmission capacity of digital subscriber lines with phantom circuit and crosstalk cancelation. *Telecommunication Systems*, 59(4), 429–436.
31. Itu-T G.993.2. (2011). Series G: Transmission systems and media, digital systems and networks: Very high speed digital subscriber line transceivers 2 (VDSL2).
32. Franco, C., Ennio, G., Paola, P., & Susanna, S. (2007). Proposal and performance evaluation of a packet over VDSL protocol for increasing throughput in the transmission of IP packets. *International Journal Communications Systems*, 17(4), 363–374.



**Chee Keong Tan** is a telecommunication engineering expert and consultant with over 10 years of experience in telecommunication research, lectures and practice. He is also an experienced speaker and teacher, having taught many highly rated university level courses, industry short courses, tutorials at conferences, to a wide range of students from industry, academia and government. Specializing in wireless system design, he has carried out projects for telecommunication companies and cellular

service providers, which led to the development of two patents on wireless algorithm and protocol design. Furthermore, he is the main contributing authors to more than 10 international journal papers, particularly on the radio resource management for various wireless systems. He holds the degrees of B.Eng. (Electronics majoring in Telecommunication), M.Eng.Sc. (wireless communications) and Ph.D. (wireless communications) from Multimedia University, Malaysia. Currently, he

serves as a senior lecturer in Faculty of Engineering, Multimedia University, Malaysia. As the lecturer in Multimedia University, he has involved in lecture for many undergraduate courses such as data communications and computer networking, analog and digital communications, mobile and satellite communications, communication networks, etc. His current research interests include radio resource management, LTE, 5G networks, cognitive radio, wireless ad hoc networks, WiMAX and mesh networking.



**Teong Chee Chuah** received the B.Eng. degree (first-class honors) in electrical and electronic engineering and the Ph.D. degree in digital communications from Newcastle University, UK, in 1999 and 2002, respectively. Since 2003, he has been with the Faculty of Engineering, Multimedia University, Malaysia. His research interests include advanced signal processing techniques and error control coding for broadband access communications. Since 2008, he

has been serving as a Technical Consultant on digital subscriber line technology to the industry.



**Mohd Saiful Bahri** is a Senior Researcher at Telekom Research & Development in Cyberjaya, Malaysia, where he is the Technical Leader of various research projects in data communication, networking and green technology. He received the B.Eng. degree in Electrical and Electronics and a M.Sc. degree in Signal & System from International Islamic University, Malaysia. Before joining Telekom Research & Development, he had served for 10 years as Senior Lead Design Engineer in the industry

and is currently involved in research for telecommunication service providers. His research interests are analytical studies and algorithm development related to Telecommunications.

Reproduced with permission of copyright owner. Further reproduction prohibited without permission.